第 28 卷第 12 期 无 机 化 学 学 报 Vol.28 No.12
2012 年 12 月 CHINESE JOURNAL OF INORGANIC CHEMISTRY 2626-2632

Mn_2O_3 微纳米粉体的配合物热解制备与电化学性质

张 防 张校刚*
(南京航空航天大学材料科学与技术学院,南京 210016)

摘要: 利用液相扩散法制备了异烟酸锰超分子配合物,通过将其在空气中高温煅烧制备了 Mn_2O_3 微纳米粉体。利用 FTIR、TG-DTA、XRD、TEM 和 FESEM 对产物进行了表征。电化学测试表明,Mn_2O_3 微纳米粉体在 0.5 mol·L^{-1} Na_2SO_4 电解液中表现出良好的电化学电容特性,在电流密度为 0.5 A·g^{-1} 时其单电极比容量可达到 88 F·g^{-1},循环 3 000 次后容量保持率可达到 80%。

关键词: Mn_2O_3 微纳米粉体; 配合物; 热解; 电化学性能
中图分类号: O614.7$^+$11; O646.54 **文献标识码**: A **文章编号**: 1001-4861(2012)12-2626-07

Mn_2O_3 Sub-Micron Powder: Preparation via Complex Thermolysis Route and Electrochemical Properties

ZHANG Fang ZHANG Xiao-Gang*
(*College of Material Science and Technology, Nanjing University of Aeronautics and Astronautics, Nanjing* 210016 *China*)

Abstract: This report describes a facile preparation and electrochemical properties of Mn_2O_3 sub-micron powder via thermal decomposition of an isonicotinic acid manganese complex. An isonicotinic acid manganese complex of $[Mn(INA)_2(H_2O)_4]_n$ (INA=isonicotinic acid) was synthesized by liquid diffusion method using an aqueous solution of manganese acetate and isonicotinic acid as the raw material. Mn_2O_3 sub-micron powder was then prepared by solid-state thermolysis of the as-synthesized INA-Mn complex at higher temperature under atmospheric pressure. The obtained products were characterized by FTIR, TG-DTA, XRD, TEM and FESEM. As an electrode material for supercapacitors, the prepared Mn_2O_3 electrode shows a strong cycle stability in 0.5 mol·g^{-1} Na_2SO_4 electrolyte and a specific capacitance of 88 F·g^{-1} at a current density of 0.5 A·g^{-1} vs. the saturated calomel electrode (SCE).

Key words: Mn_2O_3 sub-micron powder; complex; thermolysis; electrochemical properties

Manganese oxides, characterized by low cost, abundance and environmentally friendly nature, have been the focus of intense research due to their novel chemical/physical properties and potential applications in the areas of catalysis, electrochemistry and magnetic materials [1-3]. Among them, polymorphs of Mn_2O_3 are used as catalysts for removing carbon monoxide and nitrogen oxides from waste gas [4-5]. In addition, Mn_2O_3 can be used as electrode materials for rechargeable lithium battery and supercapacitors [6-8]. Mn_2O_3 materials in micro- and nanoscale are expected to display better chemical/physical properties for all kinds of practical applications in material areas.

Several methods have been used to synthesize Mn_2O_3 nanomaterials, such as solvothermal[9-10], ethanol thermal reduction of MnO_2 [11] and thermal

收稿日期:2012-04-10。收修改稿日期:2012-06-18。
江苏省自然科学基金(No.BK2011740),江苏省博士后科研资助计划(No.1001016B)资助项目。
*通讯联系人。E-mail:azhangxg@163.com

decomposition[12]. Common manganese sources such as $MnCO_3$ and MnO_2 can be used to yield Mn_2O_3 in the presence of air or ethanol through thermal decomposition. Recently, generation of metal oxides micro- and nanomaterials via thermal decomposition of metal complexes, especially metal complex based on aromatic carboxylic acid has drawn much attention due to the control of particle size, shape and crystal structure. For example, Chen et al. prepared polyhedral MnO micro- and nanoparticles [13] and symmetrical 3D CuO superstructures [14] by using appropriate carboxylic acid complexes as precursors. Salavati-Niasari et al. also reported the preparation of NiO[15] and Co_3O_4[16] nanostructures through a simple thermolysis procedure by using corresponding phthalate complexes as the precursor.

For strong coordination ability and diverse coordination modes, the reaction of isonicotinic acid (INA) with transition metal ions has been studied extensively; much effort has been devoted to design and synthesis of metal-organic framework with novel topology and property[17-19]. However, little attention has been focused on solid state synthesis of micro- and nanomaterials from metal-INA complex so far. Herein, an INA-Mn coordinated complex was synthesized by a facile diffusion method. Through thermolysis of the as-synthesized INA-Mn complex in a two-end opened horizontal tube furnace (TOTF), we prepared Mn_2O_3 sub-micron powder by calcining the INA-Mn complex at 450 ℃ in air for 2 h. Furthermore, the electrochemical properties of as-prepared Mn_2O_3 sub-micron powder were examined by cyclic voltammetry (CV), galvanostatic charge/discharge and cycle life measurements.

1 Experimental

1.1 Materials and Characterization

All chemicals were of reagent grade and were used as received. X-ray powder diffraction (XRD) patterns were acquired on a Bruker D8 powder X-ray diffractometer with graphite monochromatized Cu $K\alpha$ radiation (λ=0.154 06 nm). Thermogravimetry/differential scanning calorimetry (TG-DSC) was performed on thermogravimetry analyzer (NETZSCH STA 409) with a heating rate of 20 ℃·min^{-1} and an air flow rate of 20 mL·min^{-1}. FTIR spectra were recorded from KBr pellets in the range of 400~4 000 cm^{-1} on a Nicolet 5DX spectrometer. Elemental analysis was done by Perkin-Elmer 240 analyzer. The field emission scanning electron micrographs (FESEM) were taken on a LEO 1530 VP field emission scanning electron microscopy. The transmission electron micrographs (TEM) and energy dispersive X-ray (EDX) spectrum were taken on a FEI Tecnai-G2 transmission electron microscopy with an accelerating voltage of 200 kV.

1.2 Preparation of Mn_2O_3 sub-micron powder

The preparation of Mn_2O_3 sub-micron powder is illustrated in Scheme 1. First, isonicotinic acid manganese complex was synthesized by a modified liquid diffusion method according to the literature[20]. Equimolar quantities of isonicotinic acid (1 mmol) and $Mn(CH_3COO)_2·2H_2O$ (1 mmol) were dissolved in dimethylformamide (DMF) and water (20 mL), respectively. Then the DMF solution of isonicotic acid was added slowly into the water solution of $Mn(CH_3COO)_2·2H_2O$. The mixed solution was placed at 5 ℃ for several days. The colorless crystals were filtrated off, washed with distilled water for several times and dried at 40 ℃ in vacuum oven. Second, solid-state thermolysis process of isonicotinic acid manganese complex was performed in a conventional

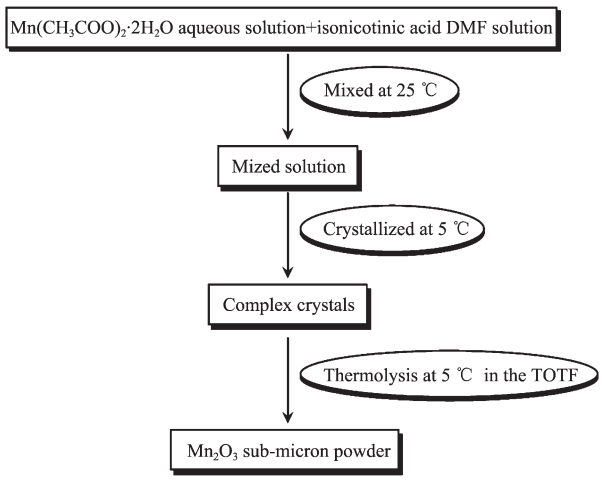

Scheme 1　Schematic illustration for the preparation of Mn_2O_3 sub-micron powder

horizontal tube furnace with both ends open to air. The as-synthesized crystals of complex were loaded into a ceramic boat, which then placed into the center of the tube furnace. Subsequently, the following parameters were set up for the thermolysis experiment: heating temperature of 450 ℃, temperature ramp of 5 ℃·min^{-1}, and holding time of 2 h. Then the furnace was shut off and cooled to room temperature naturally. Black Mn_2O_3 powder was collected for characterization.

1.3 Electrochemical Measurements of Mn_2O_3 electrode

All electrochemical measurements were performed on a CHI660 electrochemical workstation (Shanghai Chenhua Co. Ltd. China) in a three-electrode system with Pt foil as the counter electrode and a standard calomel electrode (SCE) as the reference electrode. The working electrode was prepared by mixing the active material (Mn_2O_3, 75wt%), acetylene black (20wt%) and polytetrafluoroethylene (5wt%); this mixture was then pressed onto a stainless steel expanded mesh (1 cm^2) and dried at 50 ℃. All electrodes were tested in a 0.5 mol·L^{-1} Na_2SO_4 aqueous electrolyte and all electrochemical measurements were carried out at room temperature.

2 Results and discussion

2.1 Characterization of complex precursor and Mn_2O_3 sub-micron powder

Powder X-ray diffraction (PXRD) was performed to reveal the phase purity and crystal structure of as-synthesized isonicotic acid manganese coordinated complex by comparison with the simulated pattern of INA-Mn complex formulated as $[Mn(INA)_2(H_2O)_4]_n$, based on the crystallographic data of PDF No. 28-9177 (Fig.1). It can be seen from Fig.1, the hkl faces including (001), (010), (10$\bar{1}$), (1$\bar{1}\bar{1}$), (1$\bar{1}$1), (02$\bar{1}$), (103) of the as-synthesized coordinated complex in the 2θ range of 5°~50° match well with the reported XRD pattern of $[Mn(INA)_2(H_2O)_4]_n$. The high diffraction peaks underline the fact that as-synthesized INA-Mn complex with its well defined peaks is well crystallized. Furthermore, the FTIR spectrum in Fig.2a

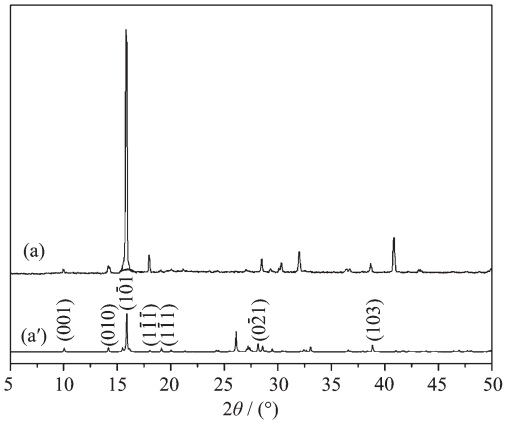

Fig.1 XRD patterns of Mn-INA complex synthesized by diffusion method (a), and simulated pattern of Mn-INA complex formulated as $[Mn(INA)_2(H_2O)_4]_n$ (a)

also demonstrates the composition of the as-synthesized INA-Mn complex. The absorption peaks of as-synthesized sample in Fig.2a is almost identical with the complex sample formulated as $[Mn(INA)_2(H_2O)_4]_n$. Elemental analysis result (%): Calcd.: C, 38.83; H, 4.34; O, 34.48; N, 7.55; Found: C, 38.79; H, 4.37; O, 34.46; N, 7.60. All the above results indicate that as-synthesized INA-Mn complex by diffusion method matches well with the reported results.

Fig.3 shows the TG-DSC curves recorded from room temperature to 600 ℃. As shown in Fig.3, two weight losses are observed. The first weight loss about 20% occurs between 100 and 130 ℃, and it is the loss of four coordinated H_2O molecules per formular

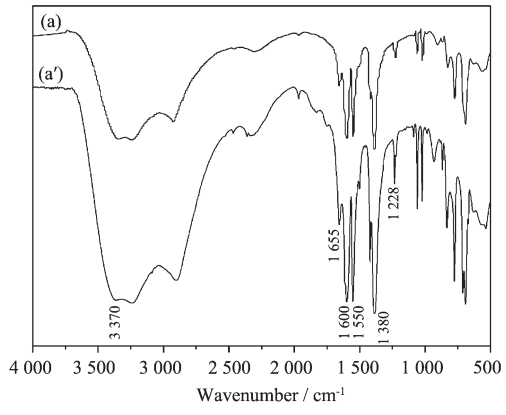

Fig.2 FTIR spectra of as-synthesized Mn-INA complex by diffusion method (a), and complex formulated as $[Mn(INA)_2(H_2O)_4]_n$ (a)

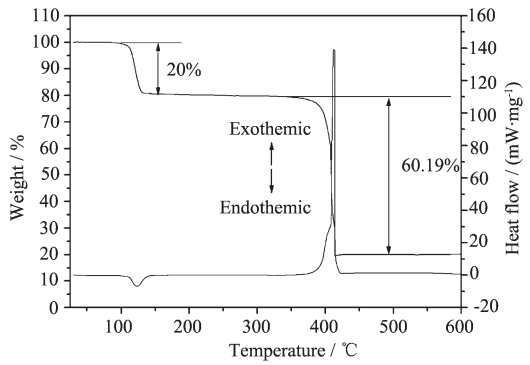

Fig.3　TG-DSC curves of as-synthesized Mn-INA complex

unit (calcd. 19.4%). Corresponding with the TG curve, a small endothermic peak is found in the DSC curve for the evaporation of water. The following weight loss occurs between 360 to 420 ℃ corresponding to the complete framework decomposition as indicated by an abrupt weight loss. Accordingly, the DSC curve shows an obvious exothermic peak for the INA-Mn complex decomposition to Mn_2O_3.

According to the TG-DSC results, the heat treatment temperature of the INA-Mn complex was set at 450 ℃ to ensure the complete decomposition. The XRD result is shown in Fig.4. All the diffraction peaks in the Fig.4 can be indexed to cubic phase Mn_2O_3 (Lattice: body-centered; Space group: *Ia*3; Cell parameters: a=0.940 91 nm; PDF No. 41-1442). No peaks from other impurities are observed, suggesting the high purity of the decomposed product.

The panoramic view of the FESEM image for the decomposed product in Fig.5a shows that the Mn_2O_3 product consists of sub-micron grains with the size

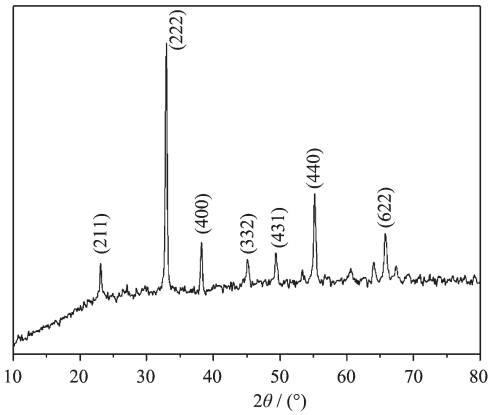

Fig.4　XRD pattern of thermal decomposed products of as-synthesized Mn-INA complex

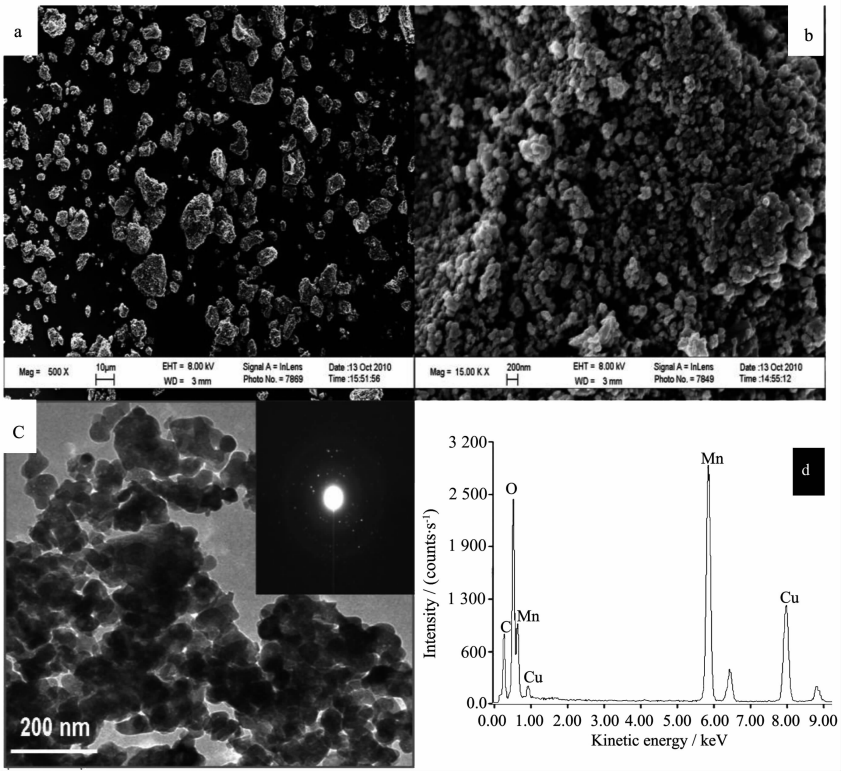

Fig.5　Typical electron micrographs of Mn_2O_3 sub-micron powder, (a, b) FE-SEM images, (c) TEM image (Right inset is ED pattern of Mn_2O_3 sub-micron powder) and (d) EDX spectrum obtained from Mn_2O_3 sub-micron powder

varying from about several to tens of micrometers. The magnified FESEM image shown in Fig.5b indicates that these primary sub-micron grains are actually assembled by a large number of agglomerate nanoparticles. From TEM images, further information about the sub-micron grains can be obtained. Fig.5c gives the typical TEM image and the corresponding selected area electron diffraction (SAED) pattern of the as-prepared sample. The product is mainly aggregates of nanoparticles with a broad size distribution, which is similar to the results in the FESEM. The SAED pattern obtained from the sample confirms the high crystallinity of these sub-micron grains. The composition of the sub-micron grains analyzed by energy-dispersive X-ray (EDX) spectroscopy is shown in Fig.5d. Only Mn and O are present in the sample (C and Cu are from the support membrane for TEM examination of the sample), atomic percent information further confirms the right stoichimetry for Mn_2O_3 crystals.

2.2 Formation mechanism of Mn_2O_3 sub-micron powder

Thermolysis of coordinated complex with metal-organic framework has been utilized to generate metal oxides micro-/nanostructures with regular shape [21-22]. Recent papers have indicated that solid-state thermolysis of coordinated complex in air actually undergoes a carbon reduction process [23-24]. When the complex is heated in tube furnace, with the increase of temperature, the coordination bond breaks and the complex precursor decomposes its organic ligands and metal ions. At higher temperature, the ligands are decomposed into carbon and different kinds of gases including hydrogen, benzene and other fragments with strong reducibility. As a typical example, Chen et al. reported the synthesis of 3D Cu superstructures from solid-state thermolysis of $[Cu_3(btc)_2]$ (btc =benzene-1,3,5-tricarboxyato)[14]. During the thermolysis process, copper ions in the complex are reduced to metallic simple substance under reducing atmosphere. When calcining the precursor for longer time, the metal Cu is further transformed into CuO. According to the literature and our results, we believe that the solid-state thermolysis of as-synthesized INA-Mn coordinated complex into Mn_2O_3 sub-micron powder in the air may include decomposition, reduction and oxidation process. Reaction temperature and time play an important role for the formation of final Mn_2O_3 products. Meanwhile, the formation of sub-micron grains is induced from the decomposition of coordinated complex related to the INA ligand and manganese ions. The further formation mechanism of Mn_2O_3 sub-micron powder is still under study.

2.3 Electrochemical properties of Mn_2O_3 sub-micron powder

Fig.6a shows the CV curves of Mn_2O_3 electrode with various scan rates in 0.5 mol·L^{-1} Na_2SO_4 electrolyte. It can be seen that the CV curves at slow scan rate exhibit fine rectangular shape, indicating the excellent reversibility and ideal electrochemical capacitive behavior of the materials. No obvious redox peaks are present in the CV curves, suggesting that the measured electrode charges and discharges at a pseudo-constant rate over the complete voltammetric cycle[25]. With the increase of scan rates, the deviation from rectangularity becomes obvious. The charge storage mechanism of Mn_2O_3 electrode in Na_2SO_4 electrolyte may be similar to MnO_2 based electrode[26].

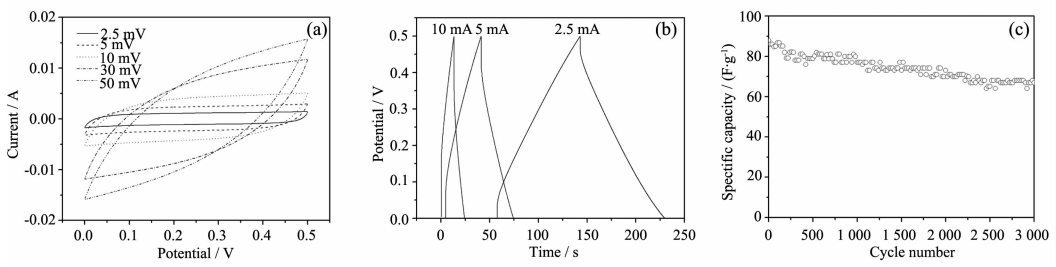

Fig.6 CV curves at various scan rates (a), CP plots at different current densities (b), and cycle number (c) of as-prepared Mn_2O_3 electrode

At slower scan rate, Na^+ from electrolyte can be inserted into almost all available pores not only on the surface but also inside of Mn_2O_3 electrode, which leads to a high effective utilization of Mn_2O_3 for the redox reaction and a high capacitance. With the increase of scan rate, the effective interaction between the ions and the electrode is greatly reduced. The effective utilization for redox reaction has been limited only to the outer surface of Mn_2O_3 electrode, leading to a reduction in capacitance.

To acquire more information for the pseudocapacitive behavior of Mn_2O_3 electrode, galvanostatic charge-discharge measurement was performed in the potential range of 0 ~0.50 V (vs. SCE). Fig.6b shows the constant current charge-discharge curves of Mn_2O_3 electrode at different current densities. A linear variation of the potential during both charging and discharging process is observed for the Mn_2O_3 electrode, which is another characteristic feature for the capacitance behavior of a material[27]. The time of charging and discharging are almost the same, which implies high reversibility and coulombic efficiency of the Mn_2O_3 electrode. The specific capacitance of the electrode at different current densities can be calculated by $(I\times t)/(V\times m)$ from the discharge curves, where I is the galvanostatic discharge current, t is the discharging time, ΔV is the potential drop during discharge and m is the mass of electroactive material (5 mg). According to the equation, the specific capacitance value of Mn_2O_3 electrode is 88, 72, and 56 $F\cdot g^{-1}$ at the current density of 0.5, 1, and 2 $A\cdot g^{-1}$, respectively. The discharge capacitance of Mn_2O_3 electrode decreases with the increase of charge-discharge current density, which is responsible for the internal resistance and polarization of the electrode[28].

The electrochemical stability was also examined by the continuous charge-discharge measurements over 3 000 cycles. Fig. 6c shows the specific capacitance variation for the Mn_2O_3 electrode as a function of cycle number at the current density of 0.5 $A\cdot g^{-1}$ within a voltage range of 0~0.5 V in 0.5 $mol\cdot L^{-1}$ Na_2SO_4 electrolyte. After 3000 cycles, a high retention rate of about 80% in specific capacitance can be seen from Fig.6c. The result indicates that the prepared Mn_2O_3 electrode has a good cycle stability in neutral electrolyte.

3 Conclusions

In summary, Mn_2O_3 sub-micron powder has been prepared via a complex-precursor thermal decomposition route. Electrochemical measurements reveal that the as-prepared Mn_2O_3 sub-micron powder could deliver a specific capacitance of 88 $F\cdot g^{-1}$ at a current density of 0.5 $A\cdot g^{-1}$ and a good cycle stability in neutral aqueous Na_2SO_4 electrolyte. The results suggest that these Mn_2O_3 sub-micron powder may have potential applications in electrochemical capacitors.

References:

[1] Du J, Gao Y Q, Li L, et al. *Nanotechnology*, **2006**,**17**:4923-4928

[2] Yu P, Zhang X, Chen Y, et al. *Mater. Chem. Phys*., **2009**, **118**:303-307

[3] Jiang H, Zhao T, Yan C Y, et al. *Nanoscale*, **2010**,**2**:2195-2198

[4] Baldi M. *Appl. Catal. B: Environ.*, **1998**,**17**:L175-L182

[5] Zang H M, Teraoka Y. *Catal. Today*, **1989**,**6**:155-162

[6] Tabuchi M, Ado K. *J. Electrochem. Soc*., **1998**,**145**:L49-L52

[7] Qiu Y C, Xu G L, Yang S H, et al. *J. Mater. Chem*., **2011**, **21**:6346-6353

[8] Nathan T, Cloke M, Prabaharan S R S. *J. Nanomater*., **2008**, **2008**:1-6

[9] Liu L, Liang H, Yang H X, et al. *Nanotechnology*, **2012**,**22**: 015603

[10]Yu S, Yoshimura M. *Adv. Mater.*, **2002**,**14**:296-300

[11]He W L, Zhang Y C, Zhang X X, et al. *J. Cryst. Growth*, **2003**,**252**:285-288

[12]Lei S J, Tang K B, Fang Z, et al. *Mater. Lett*., **2006**,**60**:53-56

[13]Chen L Y, Xing H, Shen Y M, et al. *J. Solid State Chem*., **2009**,**182**:1387-1395

[14]Chen L Y, Shen Y M, Bai J F, et al. *J. Solid State Chem*., **2009**,**182**:2298-2306

[15]Salavati-Niasari M, Mohandes F, Davar F, et al. *Inorgan. Chim. Acta*, **2009**,**362**:3691-3697

[16]Mohandes F, Davar F, Salavati-Niasari M. *J. Magn. Magn.*

Mater., **2010**,**322**:872-877

[17]Liu Y H, Lu Y L, Tsai H L, et al. *J. Solid State Chem.* **2001**,**158**:315-319

[18]Can N, Sözerli Can S E, et al. Polyhedron, **2004**,**23**:1109-1113

[19]Chapman M E, Ayyappan P, Foxman B M, et al. *Cryst. Growth Des.*, **2001**,**1**:159-163

[20]Zhang F, Zhang X G, Hao L. *Mater. Chem. Phys.*, **2001**,**126**: 853-858

[21]Li Z Q, Xie Y, Xiong Y J, et al. *New J. Chem.*, **2003**,**27**: 1518-1521

[22]Xiong Y J, Xie Y, Li Z Q, et al. *Chem. Eur. J.*, **2003**,**9**: 1645-1651

[23]Schmitt W, Hill J P, Malik S, et al. *Angew. Chem. Int. Ed.*, **2005**,**44**:7048-7053

[24]Chen L Y, Bai J F, Wang C Z, et al. *Chem. Commun.*, **2008**,**11**:1581-1583

[25]Xu M W, Kong L B, Zhou W J, et al. *J. Phys. Chem. C*, **2007**,**111**:19141-19147

[26]Devaraj S, Munichandraiah N. *J. Phys. Chem. C*, **2008**,**112**: 4406-4417

[27]Devaraj S, Munichandraiah N. *J. Electrochem. Soc.*, **2007**, **154**:A80-A88

[28]Wang Y G, Xia Y Y. *J. Electrochem. Soc.*, **2006**,**153**:A450-A454